

## Electric field quantification method for a p-n junction by DPC STEM

Toyama, S.<sup>1</sup>, Seki, T.<sup>1</sup>, Sasaki, H.<sup>2</sup>, Ikuhara, Y.<sup>1,3</sup> and Shibata, N.<sup>1,3</sup>

<sup>1</sup> The University of Tokyo, Japan, <sup>2</sup> Furukawa Electric Co. Ltd., Japan, <sup>3</sup> Japan Fine Ceramics Center, Japan

By using differential phase contrast (DPC) imaging method in scanning transmission electron microscopy (STEM), local electromagnetic fields in specimens can be observed directly in real-space at high spatial resolution [1]. In DPC STEM, deflection of electron beam due to electromagnetic fields can be detected by a segmented detector placed in the bright field (BF) region (Fig. 1). In the previous report, the estimation of center-of-mass (CoM) of diffraction pattern at each probe raster using segmented detectors was shown to be effective for DPC STEM image quantification [2]. On the other hand, phase contrast transfer function (PCTF) can be defined for DPC STEM within the domain of weak phase object approximation. It has been shown that the true electric fields can be quantitatively related to the CoM estimated by segmented detectors through the PCTF described by the lens transfer function and the detector response function [3]. Using the PCTF concept, we can eliminate the effect of finite detector sizes and shapes for DPC quantification by deconvolving the point spread function derived from the PCTF [3]. However, a large under estimation of true electric field in experiments was pointed out for a p-n junction imaging in a thick specimen [4]. The main cause of the underestimation is considered to be plasmon scattering. Plasmon scattering appears to blur the diffraction pattern on the segmented detectors and thus affect the DPC quantification. In this study, we attempt to remove the plasmon-scattering effect from DPC signals and to improve quantitativity of DPC STEM for a p-n junction in semiconductors.

Here, a model p-n junction specimen was used: a GaAs doped with  $10^{18}$  atom/cm<sup>3</sup> C for p-type region and  $10^{18}$  atom/cm<sup>3</sup> Si for n-type region. We imaged the built-in electric fields in between the p-n junction by DPC STEM using JEM-ARM300F equipped with 16-segment SAAF detector (JEOL Ltd.). Several probe sizes and probe current conditions were chosen to examine the effect of optical conditions.

First, we obtained two BF disk patterns from an uniform specimen region without p-n junction and from vacuum region (Fig. 2). Next, we deconvolved these two patterns to extract a function of the plasmon-scattering effect. The extracted function was then convoluted to the detector response function. Detecting diffraction intensity convoluted with the plasmon function by a segmented detector could be mathematically equivalent to detecting unblurred diffraction intensity by a segmented detector convoluted with the plasmon function (Fig. 3) [4]. Using this blurred detector response function, we can calculate a PCTF including the plasmon effect. Finally, deconvolving this PCTF from the experimental DPC STEM images, we can now remove the both effects of the segmented detector and the plasmon-scattering blurring. We compared thus processed DPC STEM images with electron holography using the same p-n junction specimen, and confirmed good agreement. In the presentation, detailed method will be discussed.

[1] Shibata, N., Findlay, S. D., Sasaki, H., Matsumoto, T., Sawada, H., Kohno, Y., Otomo, S., Minato, R. and Ikuhara, Y. *Sci. Rep.* **5**, 10040 (2015).

[2] Close, R., Chen, Z., Shibata, N. and Findlay, S. D. *Ultramicroscopy* **159**, 124 (2015).

[3] Seki, T., Sánchez-Santolino, G., Ishikawa, R., Findlay, S. D., Shibata, N. and Ikuhara, Y. *Ultramicroscopy* **182**, 258 (2017).

[4] Brown, H. G. Shibata, N. Sasaki, H. Petersen, T.C., Paganin, D.M., Morgan, M.J. and Findlay, S.D. *Ultramicroscopy* **182**, 169 (2017).

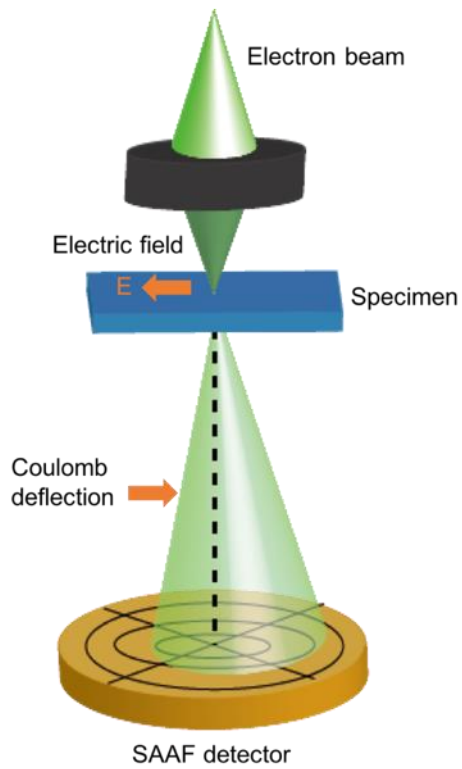


Fig. 1 Schematic image of DPC STEM.

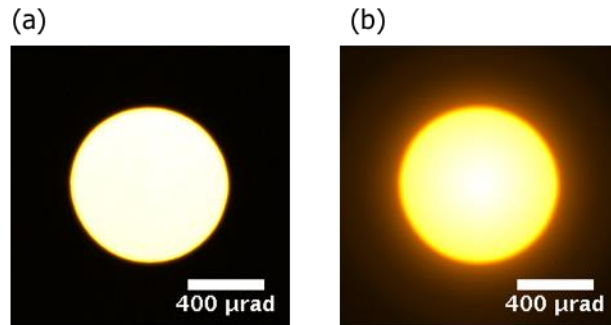


Fig. 2 (a,b) Bright field disk patterns of without and with specimen, respectively.

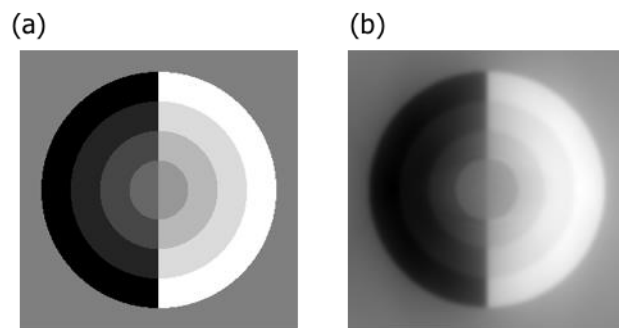


Fig. 3 (a,b) Unblurred and blurred detector response functions of lateral direction, respectively.